remote sensing

MDPI

Article

A Strict Validation of MODIS Lake Surface Water Temperature on the Tibetan Plateau

Lazhu [1,2], Kun Yang [2,3,*], Jun Qin [4], Juzhi Hou [2], Yanbin Lei [2], Junbo Wang [2], Anning Huang [5], Yingying Chen [2], Baohong Ding [2] and Xin Li [2]

1 Research Center for Ecology, College of Science, Tibet University, Lhasa 850011, China
2 Institute of Tibetan Plateau Research, Chinese Academy of Sciences, Beijing 100101, China
3 Ministry of Education Key Laboratory for Earth System Modeling, Department of Earth System Science, Tsinghua University, Beijing 100084, China
4 State Key Laboratory of Resources and Environmental Information System, Institute of Geographic Sciences and Natural Resources Research, Chinese Academy of Sciences, Beijing 100101, China
5 CMA-NJU Joint Laboratory for Climate Prediction Studies, School of Atmospheric Sciences, Nanjing University, Nanjing 210023, China
* Correspondence: yangk@tsinghua.edu.cn

Abstract: Lake surface water temperature (LSWT) is a key parameter in understanding the variability of lake thermal conditions and evaporation. The MODIS-derived LSWT is widely used as a reference for lake model validations and process studies in data-scarce regions. In this study, the accuracy of the MODIS LSWT was examined on the Tibetan Plateau (TP). In-situ subsurface temperatures were collected at five large lakes. Although the observation period covers from summer to winter, only the observations during the lake turnover period (from October to freeze-up), when the lakes are well mixed, can be used as ground truth. The MODIS LSWT agrees well with the selected in-situ data for the five large lakes, with root mean square error (RMSE) < 1 °C at nighttime and <2 °C in the daytime, indicating a high accuracy of the MODIS LSWT data. Before the turnover period, the water is thermally stratified and the surface water is warmer than the subsurface water, and thus the in-situ subsurface water temperature data and the MODIS LSWT have different representativeness. In this case, if the observations are used as a validation basis, the MODIS errors could be much magnified. This in turn indicates the importance of period selection for the validation.

Keywords: Tibetan Plateau; MODIS; lake surface water temperature; lake turnover

check for updates

Citation: L.; Yang, K.; Qin, J.; Hou, J.; Lei, Y.; Wang, J.; Huang, A.; Chen, Y.; Ding, B.; Li, X. A Strict Validation of MODIS Lake Surface Water Temperature on the Tibetan Plateau. *Remote Sens.* **2022**, *14*, 5454. https://doi.org/10.3390/rs14215454

Academic Editor: Catherine Ottlé

Received: 30 August 2022
Accepted: 25 October 2022
Published: 30 October 2022

Publisher's Note: MDPI stays neutral with regard to jurisdictional claims in published maps and institutional affiliations.

Copyright: © 2022 by the authors. Licensee MDPI, Basel, Switzerland. This article is an open access article distributed under the terms and conditions of the Creative Commons Attribution (CC BY) license (https://creativecommons.org/licenses/by/4.0/).

1. Introduction

The contrasting properties between the lake and land surfaces (e.g., their surface albedo, heat capacity and roughness length) can cause local air circulations that affect the local climate [1–5]. In particular, lake surface evaporation after the onset of the dry and cold season can increase greatly, causing heavy rainfall or snow downwind of large lakes at high latitudes and high elevations [2,6,7]. Therefore, lake–atmosphere interactions are included in the land surface schemes used in high-resolution weather/climate modeling [1,8–13]. The lake surface water temperature (LSWT) is a crucial parameter in calculating evaporation and sensible heat flux at the lake–air interface [14–18]. In addition, LSWT is widely used in lake biology and climate change studies [19,20]. However, in-situ LSWT data are often not available in remote regions such as the Tibetan Plateau.

Instead of in-situ LSWT data, satellite remote sensing data, if proven reliable, can be used as an alternative [10,11,21–23]. The Moderate Resolution Imaging Spectroradiometer (MODIS) LSWT product has been broadly validated worldwide, showing acceptable errors [24–28]. For the two largest Swedish lakes, the MODIS retrieval showed good agreement with in-situ measurements at a depth of 0.5 m, with a root mean square error (RMSE) of less than 0.50 °C [29]. At the Great Salt Lake, Utah, the MODIS-derived LSWT showed

a cold bias (−1.5 °C) and an RMSE of 1.6 °C compared to the in-situ measurements at a depth of 0.5 m [30]. A cold bias was also found at Lake Taihu, China, and the RMSE was less than 1.8 °C when compared with field measurements at depths of 0.5 to 1 m [31]. These validation studies do not pay attention to the representativeness of in-situ measurements, which could be different for different lake thermal phases.

The Tibetan Plateau (TP) has more than 1400 inland lakes with areas greater than 1 km^2, and the total area of TP lakes represents more than 50% of the inland water area in China [32]. Most of the lakes have expanded since the mid-1990s; the expansion is continuing [33,34] and represents one of the most outstanding environmental change events [35]. To better understand the response of the lake water and energy budgets to climate change on the data-scarce TP, the MODIS LSWT has been used to investigate the lake warming trends [20,36–38] and to validate the simulated bulk temperature of the mixed layer in lake modeling [22,39–42].

However, caution must be exercised regarding the accuracy of the MODIS LSWT when it is used for lake process studies on the TP. Xiao et al. [43] showed that the daytime MODIS LSWT had an RMSE of 1.5 °C at Lake Qinghai compared to the in-situ measurements at a depth of 0.5 m, but the comparison was based only on a short period of lake thermal stratification (July of 2010 and 2011). Zhang et al. [36] found that the nighttime MODIS LSWT had an unexpected high RMSE (4.5 °C) in another large lake (Lake Nam Co) using radiometric skin temperature collected near the lake shoreline, but the comparison period contained the lake ice phase during which the difference between the two data sets was large. These studies did not consider the impacts of lake stratification and attributed the difference between the MODIS LSWT and in-situ data to retrieving errors. Recently, Wan et al. [44] released a 15-year (2001–2015) time series of the daytime and nighttime MODIS LSWT for TP lakes, but the accuracy of the MODIS LSWT was not evaluated by the in-situ observations. Therefore, validation studies of the MODIS LSWT in the region are limited and even questionable; specifically, they ignored the conditions under which in-situ subsurface temperature data can be used to validate the satellite-retrieved surface temperature.

A comprehensive evaluation of the MODIS LSWT data should take the TP's unique climate and environment into account. The solar radiation over the TP is very strong [45,46] and the solar heat on the water surface may cause obvious thermal stratification. This phenomenon should be accounted for carefully, otherwise it will lead to artificially magnified errors in the MODIS LSWT. The goal of this study is to consider this phenomenon in the MODIS LSWT evaluation process and to present criteria for validations and applications of the MODIS LSWT over the TP.

In this study, buoy data at five lakes during the open-water period of a full year were used to investigate the accuracy of the MODIS LSWT data during two periods (lake stratification and turnover). The lakes and data sets (buoy data and the MODIS LSWT) are introduced in Section 2, and the comparison method is described in Section 3. The discrepancies between the MODIS LSWT and in-situ data are presented in Section 4, and the reason for the substantial underestimates in the nighttime MODIS LSWT in summer is discussed in Section 5. Finally, the results of this study are summarized in Section 6.

2. Study Area and Data Sets

The climate in the TP is dominated by the Asian monsoon during summer and early autumn, and by westerlies during other seasons. The influence of the monsoon is most prominent during July and August, and the monsoon season in this study refers to the period during July and August. The climate in northwest TP is mainly influenced by the westerlies throughout all seasons. Most lakes in the TP are located in the central and western TP and are influenced by both the monsoon and the westerlies.

2.1. Lake Locations

Subsurface water temperature data were collected for a full annual cycle at five large lakes which are located in different climate regions of the TP (Figure 1 and Table 1). The Lake Bangong Co (33.68°N, 79.22°E, 671 km^2) on the arid western TP, is an endorheic and dimictic lake. According to the meteorological data observed in 2013 at Ngari Station for Desert Environment Observation and Research, CAS (about 10 km away from Bangong Co), the mean annual air temperature is 1.2 °C with the lowest value of −26.1 °C in January, the mean annual relative humidity is 33% and the annual precipitation is 125 mm. Lake Zhari Namco (30.93°N, 85.61°E, 997 km^2) is a salt semiarid lake on the southern TP, around which the mean annual air temperature is 1.2 °C and the annual precipitation is 384 mm in 2017 [47]. Lake Dagze Co (31.89°N, 87.52°E, 295 km^2) is a brackish lake on the central TP and its salinity is 18 g/L [48]. Based on observation from Xianza Meteorological station 150 km away from the lake, the mean annual air temperature is 0.6 °C and annual precipitation is 316 mm in 2012 [48]. Lake Nam Co (30.74°N, 90.61°E, 2021 km^2) is a dimictic, deep lake, and it is the third largest lake in the TP. The weather station on the northeastern shore of Lake Nam Co (distance of about 1.5 km) shows that the mean annual air temperature and relative humidity are −1.2 °C and 55%, and annual precipitation is 488 mm in 2013, respectively [40]. Located in the central Himalayas, Lake Peiku Co (28.89°N, 85.59°E, 280 km^2) is a deep alpine lake with a mean annual air temperature of 4.4 °C in 2015/2016 and an annual precipitation varying between 150 and 200 mm [49].

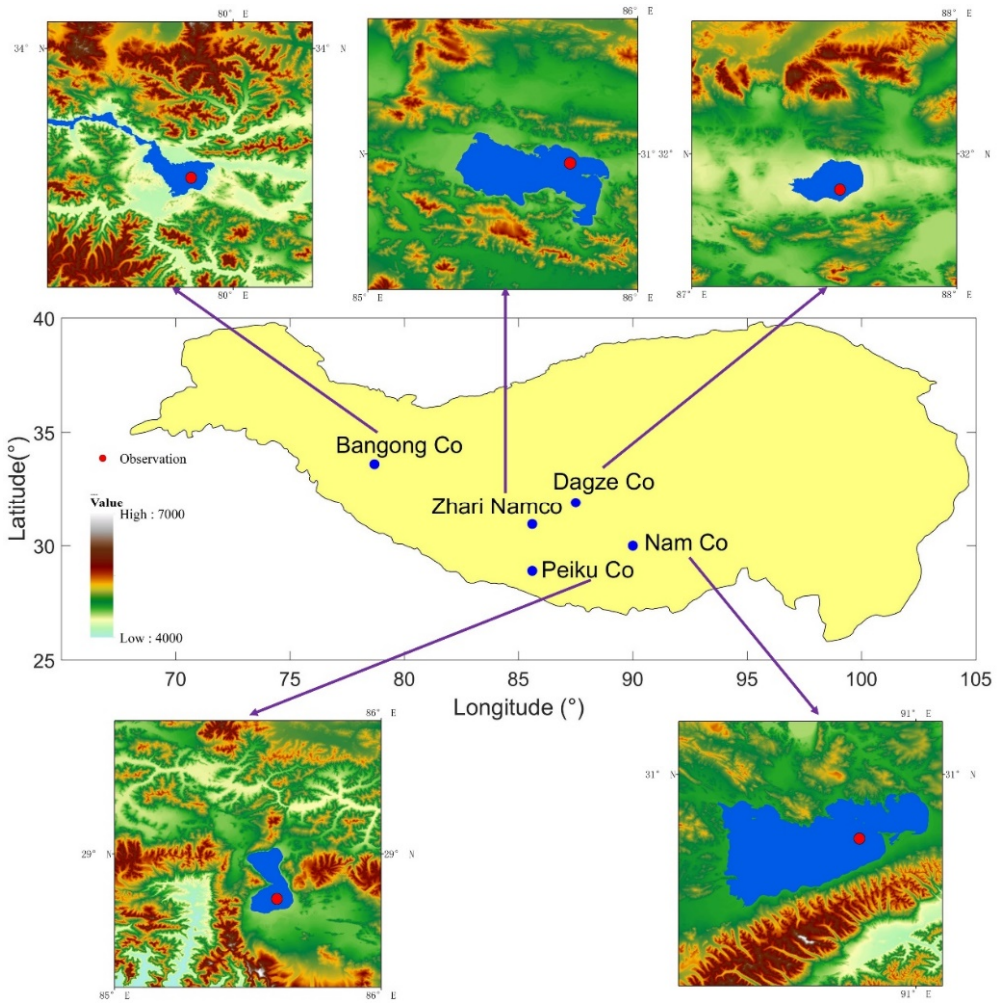


Figure 1. Location of five Tibetan Plateau lakes (Bangong Co, Zhari Namco, Dagze Co, Paiku Co, and Nam Co) and their surrounding topography (the red dots indicate water temperature monitoring stations).

Table 1. Geographical information and measurement information on the buoy stations for the five lakes. The lake depths are at the buoy stations.

Lake	Co-Ordinates	Area (km^2)	Elevation (m a.s.l)	Lake Depth (m)	Measurement Depth (m)	Motoring Sensor	Acquisition Period
Bangong Co	33.2–34.0°N 78.4–80.0°E	671	4241	36.6	5	HOBO U22-001	1 Aug 2012–31 Jul 2013
Zhari Namco	30.75–31.1°N 85.3–85.9°E	1000	4613	59.3	0.7	HOBO U22-001	1 Aug 2016–31 Jul 2017
Dagze Co	31.8–32.0°N 87.4–87.7°E	311	4450	37.3	4	HOBO U22-001	1 Sep 2012–31 Aug 2013
Nam Co	30.5–30.95°N 90.2–91.05°E	2024	4710	92.0	3	Hydrolab DS5	1 Aug 2012–31 Jul 2013
Peiku Co	28.75–29.05°N 85.45–85.7°E	280	4590	42	0.5	HOBO U22-001	1 Jun 2016–31 May 2017

2.2. In-Situ Measurements of Lake Temperature

Table 1 provides the water temperature measurement information on the buoy stations. Buoy data at Lake Nam Co were measured using a Hydrolab DS5 [50]. This probe has an accuracy of ±0.1 °C between −5 °C and 50 °C, with a resolution of 0.01 °C. Water temperatures in the other four lakes were recorded via a HOBO water temperature probe V2/U22-001 (Onset Corp., Cape Cod, USA) [48], which has a temperature range of −10 °C to 50 °C with an accuracy of ±0.2 °C and a resolution of 0.02 °C.

The measuring depths and intervals were set according to the following considerations in addition to specific reasons for the individual lakes. In previous studies [29,30], the subsurface temperatures were measured at depths shallower than 1 m. We measured temperatures at depths deeper than 1 m in some lakes to avoid destruction by ice in winter due to the lack of lake ice thickness information at the buoy sites. Specifically, subsurface temperatures were measured at depths of 5 m, 0.7 m, 4 m, 3 m and 0.5 m at these five lakes in the order shown in Table 1. The measured temperatures are able to represent the bulk temperature of the mixed layer of the lakes [48,50]. In addition, there are considerable diurnal variations in the lake surface temperature due to solar heating in the lakes' stratified period [20,26,51]. Minnett [52] recommended that validation should be conducted within ±2 h of the satellite overpass, as followed in previous studies [31,53,54]. Therefore, the buoy data in this study were collected at intervals of 1 or 2 h, and then the average within ±1 h (2 h) of the satellite overpass was sub-sampled to enable comparison between the two data sets.

According to the measurements, four of the five large lakes were completely frozen between approximately December–early January and late April–May [55,56], while the remaining one (Peiku Co) [49] was ice-free in the studied year. After the ice break-up, the lake water temperature started to increase, and the lakes became thermally stratified. The maximum water temperature occurred around late August–early September, then the temperature started to decrease, but the lakes were still stratified. From October, the upper mixed layer drastically deepened, and the lake turnover appeared before the ice cover. In this study, the lake stratified period is referred to as the period from May to September, while the lake turnover period is defined as the period from October to the freeze-up date.

2.3. MODIS Lake Surface Temperature

The MODIS level 3, 1 km nominal resolution at nadir, daily land surface temperature products (MO/YD11A1) were obtained through the NASA Level 1 and Atmosphere Archive and Distribution System (https://ladsweb.nascom.nasa.gov/data/ (accessed on 20 August 2020)). The inland lake surface temperature contained in these products was derived using thermal infrared (TIR) bands 31 and 32, and a generalized split-window algorithm. LSWT was retrieved from both platforms (Terra and Aqua) at different times on the same day. In both platforms, two instantaneous observations were collected every day (Terra: approximately 10:30 and 22:30 local time, Aqua: approximately 13:30 and 01:30 local time). The MODIS LSWT data are pre-processed to account for atmospheric and

surface emissivity effects. The cloud mask (MOD35) used for inland water provides a surface temperature measurement when there is a 66% or greater confidence of clear-sky conditions [57], otherwise no temperature measurement is produced. More details on this product were provided by Savtchenko et al. [58] and Wan et al. [59].

Satellite-derived LSWT measurements represent the instantaneous water temperature of the uppermost ∼10–20 µm deep molecular layer; this is known as the skin temperature [60,61]. However, thermometers are installed well below the lake surface and thus the measured ones are usually the bulk temperature of the mixed layer. Differences between the skin and bulk temperature are called skin effects [62–64]. As the lake thermal structure shown in Wilson et al. [64] demonstrates, the skin temperature of the upper-most layer whose thickness is less than 1 mm is controlled by heat and the momentum flux at the lake–air interface; the bulk temperature, at just a few centimeters of depth, is warmer than the skin temperature by several tenths of 1 °C due to solar heating [64,65]; for the depth of no less than 1 m, the difference between bulk temperature and skin temperature can be several degrees [27,53]. The skin effect can be impacted by solar radiation which varies with latitude and altitude, and lake thermal phases for different thermal regimes in the lake's stratified and turnover periods [27,31,66]. On the Tibetan Plateau, the stronger solar radiation in the daytime and intense longwave cooling at nighttime due to the thin air might enlarge the skin effect.

3. Methods

The MODIS level 3 daily LSWTs derived from both Terra and Aqua platforms were compared with the in-situ measurements. The MODIS LSWT at a specific lake was obtained using the MODIS Reprojection Tool (MRT, https://lpdaac.usgs.gov/tools/modis_reprojection_tool (accessed on 20 July 2019)), which involved three steps as follows.

The first step was to identify the lake water body using the MODIS land mask product at 250 m resolution (http://www.landcover.org/data/watermask/(accessed on 15 July 2019)). The land mask image was then resampled to 0.01° spatial resolution to match the resolution of the MODIS LSWT product, which was resampled to 0.01° using MRT.

The second step was data quality assurance to select LSWT data free of cloud contamination and uses the quality flag stored in quality control (QC) scientific data sets. Only pixels with quality flags designated as good quality and the average LSWT errors less than or equal to 2 K were retained.

The third step was to obtain the spatially representative MODIS LSWT data. For each lake water temperature station, a 3 × 3 pixel array centered on the monitoring station was extracted from the MODIS LSWT data, and its average LSWT was calculated for subsequent comparison with the in-situ data. Such spatial averaging is widely used for removing spatial divergence [25,29,65–67].

The selected daily MODIS LSWT data sets from Aqua and Terra were compared with the in-situ measurements at the five lakes. Given that the agreement between the observation and the MODIS data may depend on lake thermal conditions, we evaluated the daytime and nighttime MODIS LSWT in the lake stratified period and the lake turnover period, respectively. The performance of the MODIS LSWT was assessed via mean difference (MD) and root mean square difference (RMSD) between the MODIS retrievals and in-situ measurements. Finally, we investigated the impact of in-situ data from different periods and times for the evaluation of the MODIS LSWT.

4. Results

The MODIS LSWT is the lake skin temperature, whereas the in-situ data represent the bulk temperature of the mixed layer of the lakes. The MODIS LSWT was evaluated for the open-water period of a full year. When lakes were frozen (usually from January to April in large Tibetan lakes), the MODIS retrieved the ice surface temperature while the in-situ data were obtained from the subsurface water layer, so they are not comparable. Four lakes (Bangong Co, Zhari Namco, Dagze Co and Nam Co) had ice cover during the

study year, and the other one (Peiku Co) remained ice-free. The ice-covered period in the four lakes can be identified with the MODIS LSWT consequent of most of the satellite data being missing when the lake was ice-covered [68].

Figure 2 shows the comparisons between the four MODIS products (Terra and Aqua, in daytime and nighttime) and the buoy data in the five large lakes, and Figure 3 shows the error metrics of the evaluation. The open-water period consists of the lake stratified period (from May to September) and the lake turnover period (from October to the freeze-up date). As shown in Figures 2 and 3, the differences between the MODIS LSWT and in-situ data at the five large lakes are quite variable during the two periods. They were analyzed in detail in the following sub-sections.

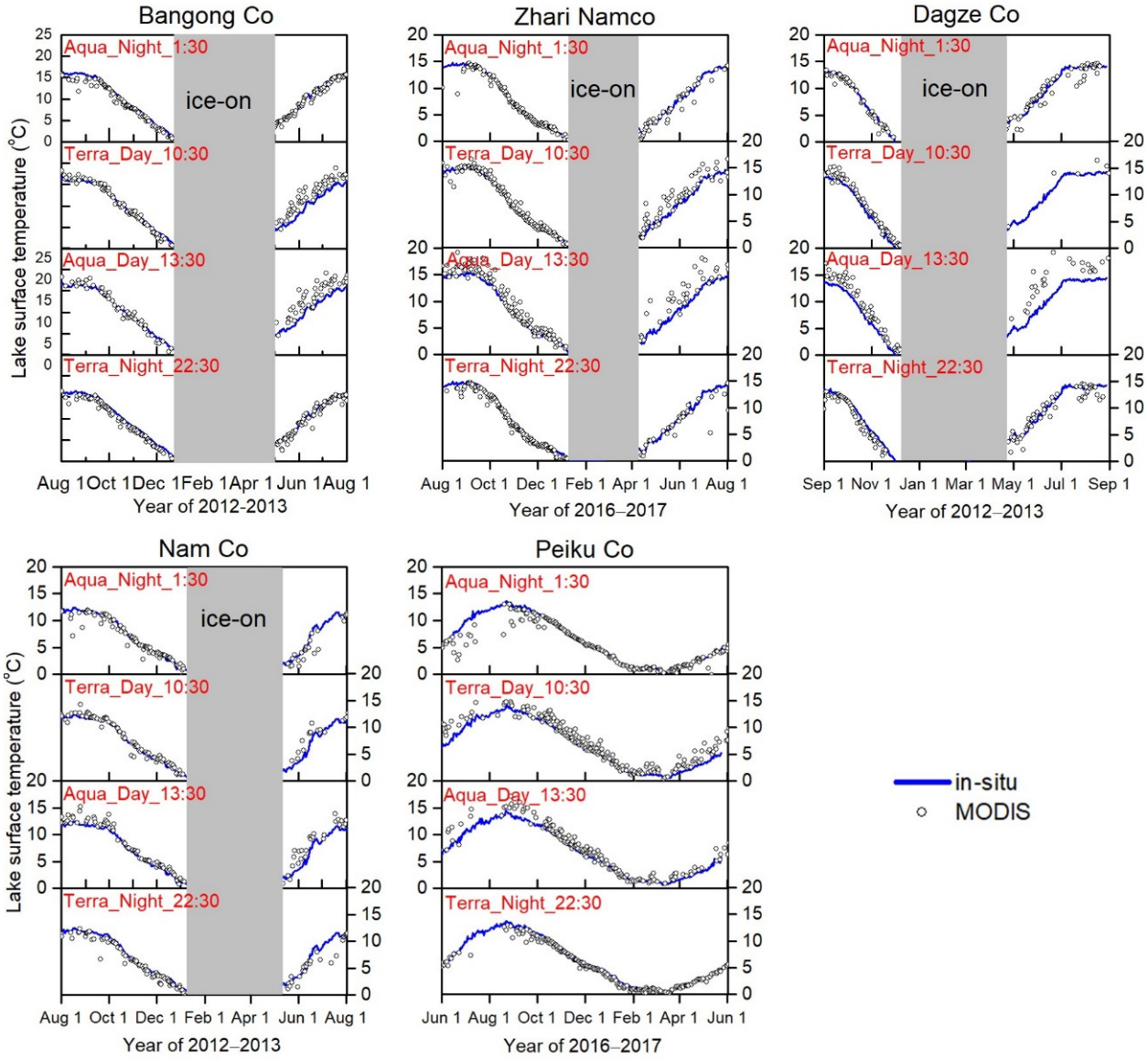


Figure 2. Comparison of daily MODIS-retrieved lake surface temperature and in-situ observed bulk temperature in the five large lakes. The four data layers for each lake represent daytime and nighttime for Terra and Aqua.

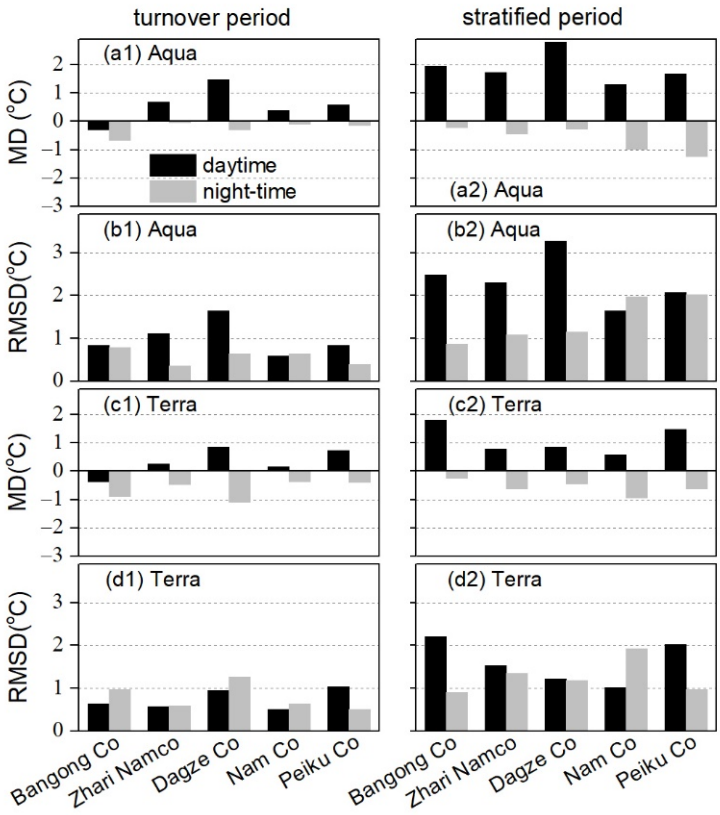


Figure 3. Mean difference (MD (**a1,a2,c1,c2**)) and root mean square difference (RMSD (**b1,b2, d1,d2**)) between MODIS LSWT and in-situ data in the daytime and at night, (1) during the lake turnover period, (2) during the lake stratified period, for Aqua (**a1,a2,b1,b2**) and Terra (**c1,c2,d1,d2**), in the five large lakes on the TP.

4.1. Results during the Lake Turnover Period

During the lake turnover period, the increased air–lake temperature gradient on the TP combined with strong wind [69,70] results in a considerable energy release from the lake to the overlying air, in terms of large latent and sensible heat fluxes as well as longwave radiation [40,71]. The lake heat loss makes the lake surface water temperature rapidly decrease, causing a sharp increase in the water density of the upper water layer, which induces vertical water convection to a large extent and eventually develops into lake turnover. As an example, Figure 4 shows that the temperature is uniform in this mixed layer. The turnover greatly reduces the difference between the surface skin temperature and the bulk water temperature, and, therefore, the subsurface temperature data can be used to validate the MODIS LSWT.

As shown in Figures 2 and 3, the MODIS LSWT is consistent with the in-situ data during this period for the five lakes, in terms of both magnitude and temporal variability. The RMSD is less than <1 °C at night and <2 °C in the daytime, indicating a high accuracy of the MODIS LSWT. The difference between the MODIS LSWT and in-situ data in Terra is relatively larger than that in Aqua, in terms of both MD and RMSD. Among the four MODIS LSWT data sets, retrieval at night from the Aqua sensor performed best in terms of consistency with the bulk temperature.

While the turnover makes the vertical water mix, the difference between the skin and bulk temperature remains. In general, the daytime MODIS LSWT is greater than the in-situ values, while the nighttime MODIS LSWT shows negligible differences from the in-situ data. The larger difference between the MODIS LSWT and the in-situ data may be due to solar heating and should not be attributed to the errors in the MODIS LSWT, as solar radiation on the TP is stronger than that along the same latitude [46,72]. To understand this, we analyzed the difference in lake temperature between the daytime and nighttime.

During this turnover period, there is strong longwave emission from the lake surface while strong solar radiation is received by the lake surface. This may cause a cooling of the surface layer at night but a warming in the daytime. This diurnal change in skin temperature can be detected by the MODIS via the Aqua platform, as shown in Figure 5a. However, the subsurface temperature of these deep lakes has a negligible response to the diurnal thermal conditions (Figure 5b) because of their huge heat capacity and high level of vertical mixing. The diurnal variation in subsurface temperature is less than that in skin temperature. Therefore, the larger MD and RMSD of the MODIS LSWT in the daytime is due to its greater representativeness in vertical differing than that of the in-situ data.

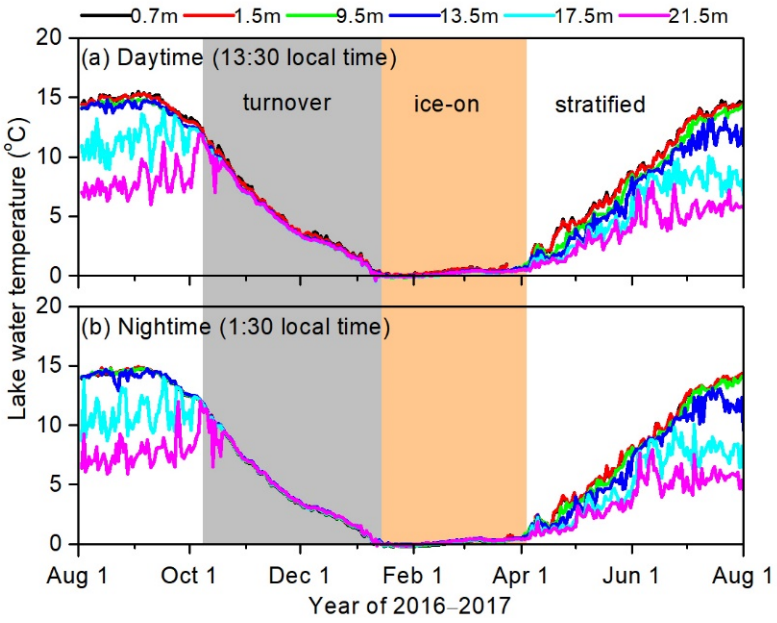


Figure 4. Observed annual cycle of thermal structure of Lake Zhari Namco in the year of 2016–2017. Water temperature was measured at five depths.

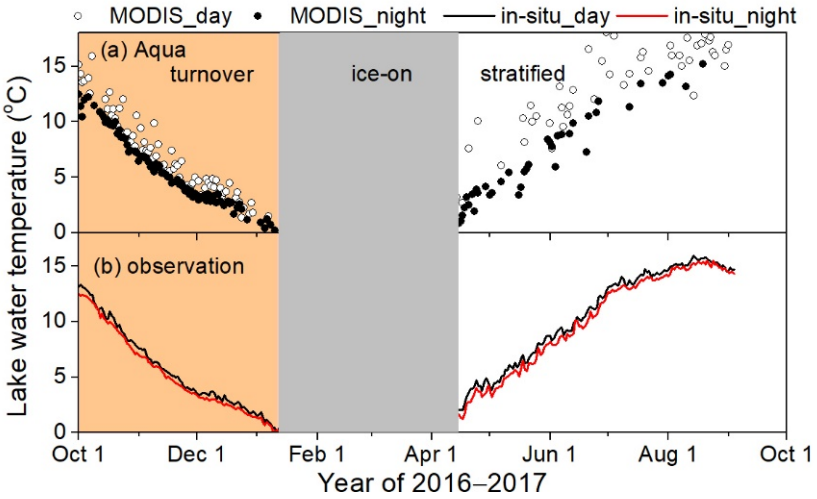


Figure 5. Time series of (**a**) MODIS retrievals and (**b**) in-situ data in the daytime and nighttime for Lake Zhari Namco in the year of 2016–2017.

Overall, the MODIS retrievals perform well during the lake turnover period for these large lakes, and using the nighttime MODIS LSWT as the ground truth for the evaluation is the most reliable.

4.2. Results during the Lake Stratified Period

At night in the lake stratified period, the MODIS LSWT from both Aqua/Terra platforms is slightly lower than the in-situ data due to the skin cooling effect of the lake, with a negative MD of less than 1 °C (Figures 2 and 3). This phenomenon is seen in both the turnover period and the stratified period. However, the RMSD in the lake stratified period is clearly larger than that in the lake turnover period (Figure 3). According to Figures 2 and 3, the MODIS Aqua has an RMSD that ranges between 0.9 °C and 2.0 °C and the MODIS Terra has an RSMD range between 0.9 °C and 1.9 °C. This is associated with the different water layer representativeness between the MODIS retrieval and the in-situ data during the summer, as discussed below.

In the daytime of the lake stratified period, the RMSD may exceed 3 °C and is larger than that at night, so our focus is the discrepancy between the MODIS retrievals and in-situ measurement in the daytime. As shown in Figure 3a2,c2, the daytime MODIS LSWT from both Aqua/Terra platforms is clearly higher than the in-situ data, as indicated by the positive MD. There are two causes for the larger errors in the daytime.

The first is the strong solar radiation in the TP. The solar heating at midday reaches its diurnal peak with a magnitude greater than 1000 Wm^{-2} [45,73]. According to the observations [74,75], the water clarity of lakes on the TP, as defined by the Secchi depth, is high: the mean is about 5 m. Therefore, most of these lakes are relatively transparent, allowing solar radiation to penetrate into deep layers. Solar radiation exponentially attenuates with water depth, which makes a large proportion of solar energy, particularly in the near-infrared band, be absorbed by the upper-most thin layer during the summer. However, as shown in Figure 4, there is a strong thermal stratification. This causes a much higher daytime MODIS LSWT than the subsurface temperature at the Aqua daytime overpass time (13:30 local time). As shown in Figure 3a2,c2, the daytime MD in Aqua is larger than 1.5 °C while in Terra it ranges between 0.6 °C and 1.8 °C.

The second is the depth of the in-situ measurements. According to the water temperature profile proposed by Wilson et al. [64], the water temperature in the subsurface layer varies rapidly with depth when the lake is thermally stratified. The depths of in-situ measurements in some lakes are considerably larger than that in other regions [25,27,31,53], therefore the measured subsurface temperature may be considerably cooler than the skin temperature due to the strong thermal stratification in the daytime.

Therefore, the representativeness in the vertical profile is different between the MODIS and the subsurface data. During the lake turnover period, the water is well mixed and the difference in representativeness is small and the evaluation result during this period is credible. However, during the stratification period, the water temperature varies with depth and the difference in representativeness is considerable; therefore, the evaluation during this period is not credible, and the difference between the in-situ data and the MODIS LSWT cannot be harshly attributed to the errors in the MODIS data.

Based on the above evaluation and reasoning, the MODIS LSWT has good accuracy for the TP lakes, with a root mean square error (RMSE) of less than 1.6 °C.

5. Discussions

Although the MODIS LSWT has good accuracy, there are still some distinct errors. Figure 2 shows some substantial underestimates in the nighttime MODIS LSWT when compared to the in-situ data during the monsoon season (summer), as also reported by Wan et al. [44]. Theoretically, the skin cooling effect at night causes the skin temperature to be slightly lower than the subsurface temperature, but it cannot explain such large cold biases at night during the monsoon season. We noticed that the large cold biases strongly depend on climate zones. For the lakes in the monsoon-controlled region (e.g., Lake Peiku Co and Lake Nam Co), some MODIS LSWTs during the monsoon season were severely underestimated. On the contrary, this situation was not so apparent for the lakes in the westerlies-dominated region (e.g., Lake Bangong Co).

During the monsoon season (from June to August), water vapor content in the monsoon-controlled region is considerably higher than in the westerly-dominated region. We speculate that the large cold biases may be related to the water vapor and cloud processes. As an example, we analyzed the relative humidity data from the observations of Lake Peiku Co, a typical lake in the monsoon region. The relative humidity data were measured at the north shoreline [76]. Figure 6a shows the temporal variations of the MODIS LSWT and in-situ measurements, Figure 6b shows the diurnal variations in relative humidity in two days with large cold biases in the MODIS LSWT and Figure 6c shows the same in the adjacent two days with small biases. It can be seen that the nighttimes with large cold biases are more humid than the ones with small biases. So, the large cold biases may be associated with the local water vapor circulation and clouds. On the TP, due to the thin air, the surface energy loss through upwelling longwave radiation is strong, causing rapid cooling of the land surface but weaker cooling of the lake surface. The resulting land–lake thermal contrast can drive cold airflow from the land to the lake surface at night. Meanwhile, evaporation from the warmer lake surface at night can replenish the water vapor in the cold air. The air convergence over the lake surface due to land wind causes upward flow. If the relative humidity is high, the upward flow may result in the condensation of water vapor. The large lakes are still at the warming stage during monsoon season (e.g., Lake Zhari Namco shown in Figure 4) and the land–lake thermal contrast is not so strong at night. Thus, upward motion over the TP's lakes is not strong enough to cause deep convections. Instead, it may cause the condensation of water vapor to form low-level fog or shallow clouds, which are usually undetectable by the MODIS sensor.

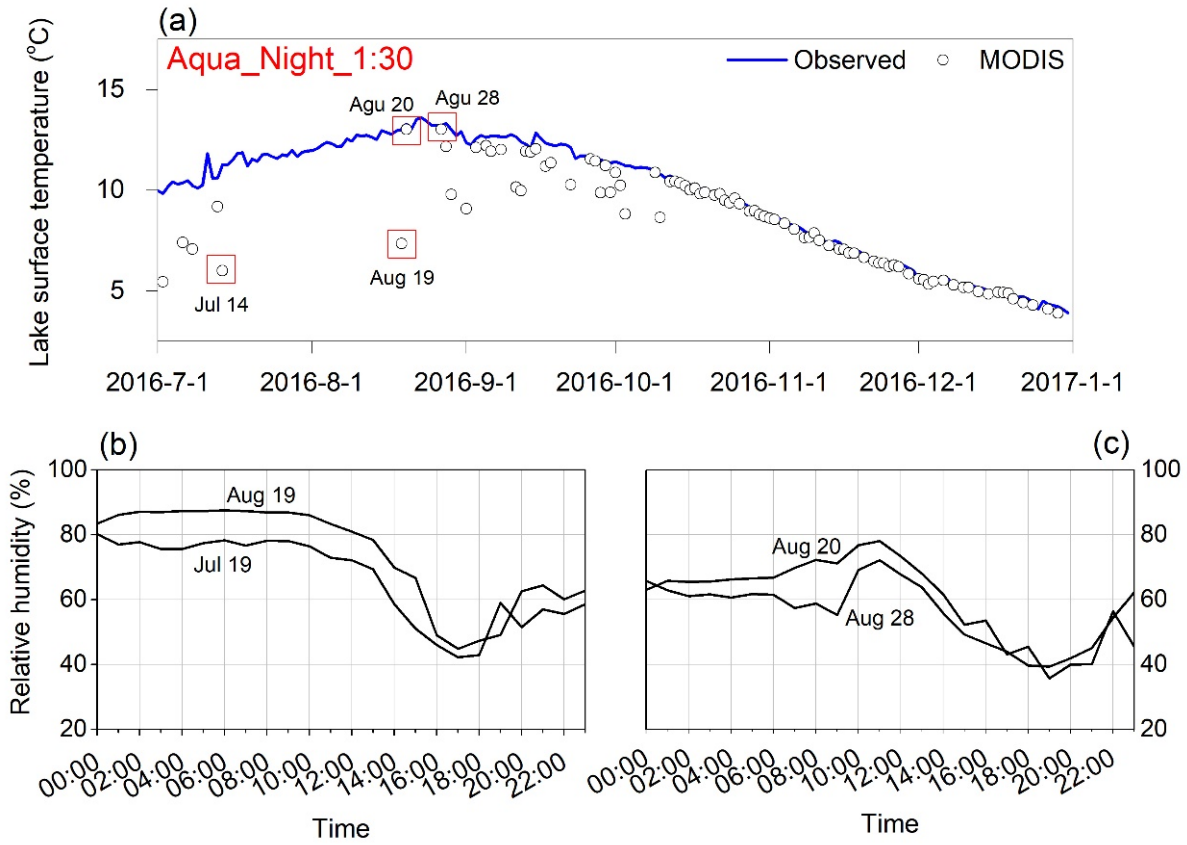


Figure 6. Comparison of MODIS Aqua and in-situ measurements of nighttime LSWT on Lake Peiku Co, (located in Himalaya region) (**a**), the diurnal variation in relative humidity on 14 July 2016 and 29 August 2016 (**b**) and 20 August 2016 and 28 August 2016 (**c**). On these two days in panel (**b**), MODIS LSWTs showed large negative deviations from the in-situ measurements, and the opposite in panel (**c**), indicated by the four red rectangles in part (**a**).

At the same time, the cloud mask criterion for the MO/YD11A1 inland water surface temperature retrieval is relatively relaxed compared to that for retrieving the land surface temperature, i.e., a water surface temperature is retrieved when the confidence of a clear-sky condition is 66% or greater, but the confidence must be greater than 99% for the land temperature retrieval [57]. In other words, the MODIS algorithm's detection of near-surface shallow clouds or fog has lower confidence. Therefore, shallow clouds and fog missing from the cloud mask might result in a considerable underestimate of nighttime LSWT during the monsoon season. Due to the lack of observational data, this speculation is subject to further confirmation in the future.

Given the frequent occurrence of large cold biases, the use of nighttime MODIS LSWT data with large cold biases during the monsoon season should be avoided in the monsoon-controlled region of the TP.

6. Conclusions

There are more than 1400 lakes with an area greater than 1 km^2 on the TP. Due to the lack of in-situ measurements, the MODIS LSWT product has been used to assess changes in lake temperature and to calculate evaporation, but the applicability of this product has remained unclear. Early limited evaluations for this region did not consider the representativeness of in-situ subsurface data, and thus may have caused uncertainties in the evaluation. In this study, we deployed buoys to measure subsurface water temperature in five large lakes on the TP and assessed the advantages and limitations of the MODIS LSWT (both Terra and Aqua) based on the buoy data. Particularly, we pay attention to the representativeness of in-situ data that varies with the seasons.

The agreement between the MODIS-derived LSWT and the in-situ observed subsurface temperature highly depends on the lake's thermal structure. During the turnover period (i.e., October to the freeze-up date), the MODIS LSWT generally shows good agreement with the in-situ data, indicating its high accuracy. Due to water mixing, the in-situ data during the nighttime of this period can be used as the ground truth in the validation of the MODIS LSWT, and the result confirms that the MODIS skin temperature can be representative of the subsurface temperature of the mixed layer of the lakes. During the lake-stratified period (from May to September), the in-situ data measured below the surface cannot represent the skin temperature detected by the MODIS LSWT and cannot be used as the ground truth for the validation of the latter.

Despite good performance in large Tibetan lakes, the MODIS lake surface temperatures can be questionable in the monsoon-controlled region. Due to the influence of the Asian monsoon, the nighttime LSWT can be heavily underestimated in the MODIS retrievals on some humid days in summer. This severely restricts the use of the MODIS LSWT on the Tibetan Plateau.

In summary, the MODIS LSWT has a high accuracy (RMSE < 2 °C) for large lakes in the TP. However, if the MODIS LSWT is assumed to represent the subsurface water temperature of a lake, it is preferable to use its nighttime data during the lake turnover period, but not to use them during the lake stratified period (especially the monsoon period).

Author Contributions: Conceptualization, L. and K.Y.; Investigation, J.H., Y.L., J.W. and Y.C.; Methodology, L., K.Y. and J.Q.; Writing—original draft, L. and K.Y.; Writing—review & editing, J.Q., A.H., Y.C., B.D. and X.L. All authors have read and agreed to the published version of the manuscript.

Funding: This work was supported by the Second Tibetan Plateau Scientific Expedition and Research Program (Grant No. 2019QZKK0206), the National Natural Science Foundation of China (Grant No. 41975125) and the Natural Science Foundation of Tibet Autonomous Region (Grant No. XZ202201ZR0046G).

Data Availability Statement: The MODIS lake surface temperature product (MO/YD11A1) was obtained through the NASA Level 1 and Atmosphere Archive and Distribution System (https://ladsweb.nascom.nasa.gov (accessed on 20 August 2020)). The in-situ measurements of lake water

temperature for Lake Bangong Co, Lake Dagze Co and Lake Nam Co can be obtained from National Tibetan Plateau Data Center (http://data.tpdc.ac.cn/en/ (accessed on 20 August 2020)).

Acknowledgments: We are grateful to everyone who participated in the field campaign establishing lake water temperature stations. We are also grateful to Ngari Station for Desert Environment Observation and Research for providing the station data and the reviewers for their invaluable comments on the manuscript.

Conflicts of Interest: The authors declare that they have no conflict of interest.

References

1. Dutra, E.; Stepanenko, V.M.; Balsamo, G.; Viterbo, P.; Miranda, P.; Mironov, D.; Schär, C. An offline study of the impact of lakes on the performance of the ECMWF surface scheme. *Boreal Environ. Res.* **2010**, *15*, 100–112.
2. Lofgren, B.M. Simulated Effects of Idealized Laurentian Great Lakes on Regional and Large-Scale Climate. *J. Clim.* **1997**, *10*, 2847–2858. [CrossRef]
3. Long, Z.; Perrie, W.; Gyakum, J.; Caya, D.; Laprise, R. Northern lake impacts on local seasonal climate. *J. Hydrometeorol.* **2007**, *8*, 881–896. [CrossRef]
4. Thiery, W.; Davin, E.L.; Panitz, H.J.; Demuzere, M.; Lhermitte, S.; Van Lipzig, N. The impact of the African Great Lakes on the regional climate. *J. Clim.* **2015**, *28*, 4061–4085. [CrossRef]
5. Yao, X.; Yang, K.; Zhou, X.; Wang, Y.; Lazhu; Chen, Y.; Lu, H. Surface friction contrast between water body and land enhances precipitation downwind of a large lake in Tibet. *Clim. Dyn.* **2021**, *56*, 2113–2126. [CrossRef]
6. Li, M.; Ma, Y.; Hu, Z.; Ishikawa, H.; Oku, Y. Snow distribution over the Namco lake area of the Tibetan Plateau. *Hydrol. Earth Syst. Sci.* **2009**, *13*, 2023–2030. [CrossRef]
7. Zhao, Z.; Huang, A.; Ma, W.; Wu, Y.; Wen, L.; La, Z.; Gu, C. Effects of Lake Nam Co and surrounding terrain on extreme precipitation over Nam Co basin, Tibetan Plateau: A case study. *J. Geophys. Res. Atmos.* **2022**, *127*, e2021JD036190. [CrossRef]
8. Balsamo, G.; Salgado, R.; Dutra, E.; Boussetta, S.; Stockdale, T.; Potes, M. On the contribution of lakes in predicting near-surface temperature in a global weather forecasting model. *Tellus A Dyn. Meteorol. Oceanogr.* **2012**, *64*, 15829. [CrossRef]
9. Dai, Y.; Wei, N.; Huang, A.; Zhu, S.; Shangguan, W.; Yuan, H.; Zhang, S.; Liu, S. The lake scheme of the Common Land Model and its performance evaluation. *Chin. Sci. Bull.* **2018**, *63*, 3002–3021. [CrossRef]
10. Gu, H.; Jin, J.; Wu, Y.; Ek, M.B.; Subin, Z.M. Calibration and validation of lake surface temperature simulations with the coupled WRF-lake model. *Clim. Chang.* **2013**, *129*, 471–483. [CrossRef]
11. Stepanenko, V.; Jöhnk, K.D.; Machulskaya, E.; Perroud, M.; Subin, Z.; Nordbo, A.; Mammarella, I.; Mironov, D. Simulation of surface energy fluxes and stratification of a small boreal lake by a set of one-dimensional models. *Tellus A Dyn. Meteorol. Oceanogr.* **2014**, *66*, 21389. [CrossRef]
12. Subin, Z.M.; Riley, W.J.; Mironov, D. An improved lake model for climate simulations: Model structure, evaluation, and sensitivity analyses in CESM1. *J. Adv. Model Earth Syst.* **2012**, *4*, M02001. [CrossRef]
13. Wen, L.; Lv, S.; Li, Z.; Zhao, L.; Nagabhatla, N. Impacts of the two biggest lakes on local temperature and precipitation in the Yellow River source region of the Tibetan Plateau. *Adv. Meteorol.* **2015**, *2015*, 248031. [CrossRef]
14. Dutton, J.A.; Bryson, R.A. Heat Flux in Lake Mendota 1. *Limnol. Oceanogr.* **1962**, *7*, 80–97. [CrossRef]
15. Lewis, W.M., Jr. Temperature, heat, and mixing in Lake Valencia, Venezuela 1. *Limnol. Oceanogr.* **1983**, *28*, 273–286. [CrossRef]
16. Magee, M.R.; Wu, C.H. Response of water temperatures and stratification to changing climate in three lakes with different morphometry. *Hydrol. Earth Syst. Sci.* **2017**, *21*, 6253–6274. [CrossRef]
17. Pour, H.K.; Rontu, L.; Duguay, C.; Eerola, K.; Kourzeneva, E. Impact of satellite-based lake surface observations on the initial state of HIRLAM. Part II: Analysis of lake surface temperature and ice cover. *Tellus A Dyn. Meteorol. Oceanogr.* **2014**, *66*, 21395. [CrossRef]
18. Verburg, P.; Antenucci, J.P. Persistent unstable atmospheric boundary layer enhances sensible and latent heat loss in a tropical great lake: Lake Tanganyika. *J. Geophys. Res.* **2010**, *115*, D11109. [CrossRef]
19. Woolway, R.I.; Kraemer, B.; Zscheischler, J.; Albergel, C. Compound hot temperature and high chlorophyll extreme events in global lakes. *Environ. Res. Lett.* **2021**, *16*, 094013. [CrossRef]
20. Ke, L.; Song, C. Remotely sensed surface temperature variation of an inland saline lake over the central Qinghai–Tibet Plateau. *ISPRS J. Photogramm. Remote Sens.* **2014**, *98*, 157–167. [CrossRef]
21. Fang, X.; Stefan, H.G. Long-term lake water temperature and ice cover simulations/measurements. *Cold Reg. Sci. Technol.* **1996**, *24*, 289–304. [CrossRef]
22. Huang, A.; Lazhu; Wang, J.; Dai, Y.; Yang, K.; Wei, N.; Wen, J.; Wu, Y.; Zhu, X.; Zhang, X.; et al. Evaluating and improving the performance of three 1-D Lake models in a large deep Lake of the central Tibetan Plateau. *J. Geophys. Res. Atmos.* **2019**, *124*, 3143–3167. [CrossRef] [PubMed]
23. Pour, H.K.; Duguay, C.R.; Martynov, A.; Brown, L.C. Simulation of surface temperature and ice cover of large northern lakes with 1-D models: A comparison with MODIS satellite data and in situ measurements. *Tellus A Dyn. Meteorol. Oceanogr.* **2012**, *64*, 17614. [CrossRef]
24. Chavula, G.; Brezonik, P.; Thenkabail, P.; Johnson, T.; Bauer, M. Estimating the surface temperature of Lake Malawi using AVHRR and MODIS satellite imagery. *Phys. Chem. Earth* **2009**, *34*, 749–754. [CrossRef]

25. Hook, S.J.; Vaughan, R.G.; Tonooka, H.; Schladow, S.G. Absolute radiometric in-flight validation of mid infrared and thermal infrared data from ASTER and MODIS on the Terra spacecraft using the Lake Tahoe, CA/NV, USA, automated validation site. *IEEE Trans. Geosci. Remote Sens.* **2007**, *45*, 1798–1807. [CrossRef]
26. Pareeth, S.; Salmaso, N.; Adrian, R.; Neteler, M. Homogenised daily lake surface water temperature data generated from multiple satellite sensors: A long-term case study of a large sub-Alpine lake. *Sci. Rep.* **2016**, *6*, 31251. [CrossRef]
27. Pour, H.K.; Duguay, C.R.; Solberg, R.; Rudjord, Ø. Impact of satellite-based lake surface observations on the initial state of HIRLAM. Part I: Evaluation of remotely-sensed lake surface water temperature observations. *Tellus A Dyn. Meteorol. Oceanogr.* **2014**, *66*, 21534. [CrossRef]
28. Tavares, M.H.; Cunha, A.H.F.; Motta-Marques, D.; Ruhoff, A.L.; Cavalcanti, J.R.; Fragoso, C.R.; Bravo, J.M.; Munar, A.M.; Fan, F.M.; Rodrigues, L.H.R. Comparison of Methods to Estimate Lake-Surface-Water Temperature Using Landsat 7 ETM+ and MODIS Imagery: Case Study of a Large Shallow Subtropical Lake in Southern Brazil. *Water* **2019**, *11*, 168. [CrossRef]
29. Reinart, A.; Reinhold, M. Mapping surface temperature in large lakes with MODIS data. *Remote Sens. Environ.* **2008**, *112*, 603–611. [CrossRef]
30. Crosman, E.T.; Horel, J.D. MODIS-derived surface temperature of the Great Salt Lake. *Remote Sens. Environ.* **2009**, *113*, 73–81. [CrossRef]
31. Liu, G.; Ou, W.; Zhang, Y.; Wu, T.; Zhu, G.; Shi, K.; Qin, B. Validating and mapping surface water temperatures in Lake Taihu: Results from MODIS land surface temperature products. *IEEE J. Sel. Top. Appl. Earth Obs. Remote Sens.* **2015**, *8*, 1230–1244. [CrossRef]
32. Zhang, G.; Luo, W.; Chen, W.; Zheng, G. A robust but variable lake expansion on the Tibetan Plateau. *Sci. Bull.* **2019**, *64*, 1306–1309. [CrossRef]
33. Zhu, L.; Xie, M.; Wu, Y. Quantitative analysis of lake area variations and the influence factors from 1971 to 2004 in the Nam Co basin of the Tibetan Plateau. *Chin. Sci. Bull.* **2010**, *55*, 1294–1303. [CrossRef]
34. Lei, Y.; Yao, T.; Bird, B.W.; Yang, K.; Zhai, J.; Sheng, Y. Coherent lake growth on the central Tibetan Plateau since the 1970s: Characterization and attribution. *J. Hydrol.* **2013**, *483*, 61–67. [CrossRef]
35. Yang, K.; Lu, H.; Yue, S.; Zhang, G.; Lei, Y.; La, Z.; Wang, W. Quantifying recent precipitation change and predicting lake expansion in the Inner Tibetan Plateau. *Clim. Chang.* **2018**, *147*, 149–163. [CrossRef]
36. Zhang, G.; Yao, T.; Xie, H.; Qin, J.; Ye, Q.; Dai, Y.; Guo, R. Estimating surface temperature changes of lakes in the Tibetan Plateau using MODIS LST data. *J. Geophys. Res. Atmos.* **2014**, *119*, 8552–8567. [CrossRef]
37. Song, K.; Wang, M.; Du, J.; Yuan, Y.; Ma, J.; Wang, M.; Mu, G. Spatiotemporal variations of lake surface temperature across the Tibetan Plateau using MODIS LST product. *Remote Sens.* **2016**, *8*, 854. [CrossRef]
38. Wan, W.; Zhao, L.; Xie, H.; Liu, B.; Li, H.; Cui, Y.; Ma, Y.; Hong, Y. Lake Surface Water Temperature Change Over the Tibetan Plateau From 2001 to 2015: A Sensitive Indicator of the Warming Climate. *Geophys. Res. Lett.* **2018**, *45*, 11–177. [CrossRef]
39. Haginoya, S.; Fujii, H.; Kuwagata, T.; Xu, J.; Ishigooka, Y.; Kang, S.; Zhang, Y. Air-lake interaction features found in heat and water exchanges over Nam Co on the Tibetan Plateau. *Sci. Online Lett. Atmos.* **2009**, *5*, 172–175. [CrossRef]
40. Lazhu; Yang, K.; Wang, J.; Lei, Y.; Chen, Y.; Zhu, L.; Ding, B.; Qin, J. Quantifying evaporation and its decadal change for Lake Nam Co, central Tibetan Plateau. *J. Geophys. Res. Atmos.* **2016**, *121*, 7578–7591. [CrossRef]
41. Zhang, Q.; Jin, J.; Zhu, L.; Lu, S. Modelling of Water Surface Temperature of Three Lakes on the Tibetan Plateau using a Physically Based Lake Model. *Atmos. Ocean* **2018**, *56*, 289–295. [CrossRef]
42. Zhou, J.; Wang, L.; Zhang, Y.; Guo, Y.; Li, X.; Liu, W. Exploring the water storage changes in the largest lake (Selin Co) over the Tibetan Plateau during 2003–2012 from a basin-wide hydrological modeling. *Water Resour. Res.* **2015**, *51*, 8060–8086. [CrossRef]
43. Xiao, F.; Ling, F.; Du, Y.; Feng, Q.; Yan, Y.; Chen, H. Evaluation of spatial-temporal dynamics in surface water temperature of Qinghai Lake from 2001 to 2010 by using MODIS data. *J. Arid Land* **2013**, *5*, 452–464. [CrossRef]
44. Wan, W.; Li, H.; Xie, H.; Hong, Y.; Long, D.; Zhao, L.; Han, Z.; Cui, Y.; Liu, B.; Wang, C.; et al. A comprehensive data set of lake surface water temperature over the Tibetan Plateau derived from MODIS LST products 2001–2015. *Sci. Data* **2017**, *4*, 170095. [CrossRef]
45. Yang, K.; He, J.; Tang, W.; Qin, J.; Cheng, C.C. On downward shortwave and longwave radiations over high altitude regions: Observation and modeling in the Tibetan Plateau. *Agric. For. Meteorol.* **2010**, *150*, 38–46. [CrossRef]
46. Tang, W.; Yang, K.; Qin, J.; Min, M. Development of a 50-year daily surface solar radiation dataset over China. *Sci. China-Earth Sci.* **2013**, *56*, 1555–1565. [CrossRef]
47. Pubu, C.; Baima, Y.; Laba, Z.; Luosang, Q.; Zheng, W. Lake Area Variation of Tharinamtso during 2002 to 2017. *Plateau Mt. Meteorol. Res.* **2018**, *4*, 67–70. (In Chinese)
48. Wang, M.; Hou, J.; Lei, Y. Classification of Tibetan lakes based on variations in seasonal lake water temperature. *Chin. Sci. Bull.* **2014**, *59*, 4847–4855. [CrossRef]
49. Lei, Y.; Yao, T.; Yang, K.; Bird, B.W.; Tian, L.; Zhang, X.; Wang, W.; Xiang, Y.; Dai, Y.; Lazhu; et al. An integrated investigation of lake storage and water level changes in the Paiku Co basin, central Himalayas. *J. Hydrol.* **2018**, *562*, 599–608. [CrossRef]
50. Wang, J.; Huang, L.; Ju, J.; Daut, G.; Wang, Y.; Ma, Q.; Zhu, L.; Haberzettl, T.; Baade, J.; Mäusbacher, R. Spatial and temporal variations in water temperature in a high-altitude deep dimictic mountain lake (Nam Co), central Tibetan Plateau. *J. Great Lakes Res.* **2019**, *45*, 212–223. [CrossRef]
51. Sharma, S.; Gray, D.K.; Read, J.S.; O'Reilly, C.M.; Schneider, P.; Qudrat, A.; Gries, C.; Stefanoff, S.; Hampton, S.E.; Hook, S.; et al. A global database of lake surface temperatures collected by in situ and satellite methods from 1985–2009. *Sci. Data* **2015**, *2*, 150008. [CrossRef] [PubMed]

52. Minnett, P.J. Consequences of sea surface temperature variability on the validation and applications of satellite measurements. *J. Geophys. Res. Oceans* **1991**, *96*, 18475–18489. [CrossRef]
53. Oesch, D.C.; Jaquet, J.M.; Hauser, A.; Wunderle, S. Lake surface water temperature retrieval using advanced very high resolution radiometer and Moderate Resolution Imaging Spectroradiometer data: Validation and feasibility study. *J. Geophys. Res. Oceans* **2005**, *110*, C12014. [CrossRef]
54. Oesch, D.; Jaquet, J.M.; Klaus, R.; Schenker, P. Multi-scale thermal pattern monitoring of a large lake (Lake Geneva) using a multi-sensor approach. *Int. J. Remote Sens.* **2008**, *29*, 5785–5808. [CrossRef]
55. Cai, Y.; Ke, C.; Li, X.; Zhang, G.; Duan, Z.; Lee, H. Variations of lake ice phenology on the Tibetan Plateau from 2001 to 2017 based on MODIS data. *J. Geophys. Res. Atmos.* **2019**, *124*, 825–843. [CrossRef]
56. Kropácek, J.; Maussion, F.; Chen, F.; Hoerz, S.; Hochschild, V. Analysis of ice phenology of lakes on the Tibetan Plateau from MODIS data. *Cryosphere* **2013**, *7*, 287. [CrossRef]
57. Wan, Z. *Collection-6 MODIS Land Surface Temperature Products Users' Guide*; ICESS, University of California: Santa Barbara, CA, USA, 2013.
58. Savtchenko, A.; Ouzounov, D.; Ahmad, S.; Acker, J.; Leptoukh, G.; Koziana, J.; Nickless, D. Terra and Aqua MODIS products available from NASA GES DAAC. *Adv. Space Res.* **2004**, *34*, 710–714. [CrossRef]
59. Wan, Z.; Zhang, Y.; Zhang, Q.; Li, Z. Quality assessment and validation of the MODIS global land surface temperature. *Int. J. Remote Sens.* **2004**, *25*, 261–274. [CrossRef]
60. Robinson, I.S.; Wells, N.C.; Charnock, H. The sea surface thermal boundary layer and its relevance to the measurement of sea surface temperature by airborne and spaceborne radiometers. *Int. J. Remote Sens.* **1984**, *5*, 19–45. [CrossRef]
61. Schluessel, P.; Emery, W.J.; Grassl, H.; Mammen, T. On the bulk-skin temperature difference and its impact on satellite remote sensing of sea surface temperature. *J. Geophys. Res. Oceans* **1990**, *95*, 13341–13356. [CrossRef]
62. Donlon, C.J.; Nightingale, T.J.; Sheasby, T.; Turner, J.; Robinson, I.S.; Emergy, W.J. Implications of the oceanic thermal skin temperature deviation at high wind speed. *Geophys. Res. Lett.* **1999**, *26*, 2505–2508. [CrossRef]
63. Donlon, C.J.; Minnett, P.J.; Gentemann, C.; Nightingale, T.J.; Barton, I.J.; Ward, B.; Murray, M.J. Toward improved validation of satellite sea surface skin temperature measurements for climate research. *J. Clim.* **2002**, *15*, 353–369. [CrossRef]
64. Wilson, R.C.; Hook, S.J.; Schneider, P.; Schladow, S.G. Skin and bulk temperature difference at Lake Tahoe: A case study on lake skin effect. *J. Geophys. Res. Atmos.* **2013**, *118*, 10–332. [CrossRef]
65. Hook, S.J.; Prata, F.J.; Alley, R.E.; Abtahi, A.; Richards, R.C.; Schladow, S.G.; Pálmarsson, S. Retrieval of lake bulk and skin temperatures using Along-Track Scanning Radiometer (ATSR-2) data: A case study using Lake Tahoe, California. *J. Atmos. Ocean. Technol.* **2003**, *20*, 534–548. [CrossRef]
66. Schneider, P.; Hook, S.J.; Radocinski, R.G.; Corlett, G.K.; Hulley, G.C.; Schladow, S.G.; Steissberg, T.E. Satellite observations indicate rapid warming trend for lakes in California and Nevada. *Geophys. Res. Lett.* **2009**, *36*, L22402. [CrossRef]
67. Schneider, P.; Hook, S.J. Space observations of inland water bodies show rapid surface warming since 1985. *Geophys. Res. Lett.* **2010**, *37*, L22405. [CrossRef]
68. Lazhu; Yang, K.; Hou, J.; Wang, J.; Lei, Y.; Zhu, L.; Chen, Y.; Wang, M.; He, X. A new finding on the prevalence of rapid water warming during lake ice melting on the Tibetan Plateau. *Sci. Bull.* **2021**, *66*, 2358–2361. [CrossRef]
69. Li, Z.; Lyu, S.; Ao, Y.; Wen, L.; Zhao, L.; Wang, S. Long-term energy flux and radiation balance observations over Lake Ngoring, Tibetan Plateau. *Atmos. Res.* **2015**, *155*, 13–25. [CrossRef]
70. Wang, B.; Ma, Y.; Ma, W.; Su, Z. Physical controls on half-hourly, daily, and monthly turbulent flux and energy budget over a high-altitude small lake on the Tibetan Plateau. *J. Geophys. Res. Atmos.* **2017**, *122*, 2289–2303. [CrossRef]
71. Li, X.; Ma, Y.; Huang, Y.; Hu, X.; Wu, X.; Wang, P.; Li, G.Y.; Zhang, S.Y.; Wu, H.W.; Jiang, Z.Y.; et al. Evaporation and surface energy budget over the largest high-altitude saline lake on the Qinghai-Tibet Plateau. *J. Geophys. Res. Atmos.* **2016**, *121*, 10–470. [CrossRef]
72. Tang, W.; Yang, K.; Qin, J.; Li, X.; Niu, X. A 16-year dataset (2000–2015) of high-resolution (3 h, 10 km) global surface solar radiation. *Earth Syst. Sci. Data* **2019**, *11*, 1905–1915. [CrossRef]
73. Li, Z.; Lyu, S.; Wen, L.; Zhao, L.; Ao, Y.; Wang, S. Effect of a cold, dry air incursion on atmospheric boundary layer processes over a high-altitude lake in the Tibetan Plateau. *Atmos. Res.* **2017**, *185*, 32–43. [CrossRef]
74. Liu, C.; Zhu, L.; Li, J.; Wang, J.; Ju, J.; Qiao, B.; Ma, Q.; Wang, S. The increasing water clarity of Tibetan lakes over last 20 years according to MODIS data. *Remote Sens. Environ.* **2021**, *253*, 112199. [CrossRef]
75. Liu, C.; Zhu, L.; Wang, J.; Ju, J.; Ma, Q.; Qiao, B.; Wang, Y.; Xu, T.; Chen, H.; Kou, Q.Q.; et al. In-situ water quality investigation of the lakes on the Tibetan Plateau. *Sci. Bull.* **2021**, *66*, 1727–1730. [CrossRef]
76. Lei, Y.; Yao, T.; Yang, K.; Lazhu; Ma, Y.; Bird, B.W. Contrasting hydrological and thermal intensities determine seasonal lake-level variations—A case study at Paiku Co on the southern Tibetan Plateau. *Hydrol. Earth Syst. Sci.* **2021**, *25*, 3163–3177. [CrossRef]